A comparative study between feedforward control and iterative learning control for trajectory tracking of Delta robot

Chems Eddine Boudjedir [1*], *Djamel* Boukhetala [1], and *Mohamed* Bouri [2]

[1]Process Control Laboratory, Ecole Nationale Polytechnique 10 Avenue des Frères Oudek, BP 182, El Harrach, 16200, El Harrach Algiers, Algeria.
[2]Laboratory of Biorobotics (BIOROB), Ecole Polytechnique Fédérale de Lausanne (EPFL), Station 9, Lausanne CH-1015, Switzerland

Abstract. This paper presents a comparative study between feedforward control (FF) and iterative learning control (ILC) with application to a parallel Delta robot performing repetitive trajectory. In order to improve the tracking trajectory of the Delta robot, a model-based feedforward compensation combined with the proportional derivative (PD) controller is introduced. As the Delta robot is affected by important frictions that are not taken into account in the dynamic model, the performance of the FF can be degraded considerably. To overcome these issues, a model-free control represented by the PD-type ILC controller is used instead the FF compensation. Experimental results show that the two strategies can ensure good tracking performance with better accuracy of ILC.

1 Introduction

Robot manipulators have been applied increasingly in the industry during the past decades, thanks to their high quality of manufacturing. Indeed, many robots have been designed to satisfy the different required tasks such as the Stewart plate form, and the Delta robot [1].

Much research has been conducted to solve the trajectory tracking problem of robot manipulators. Starting with PD controller which was developed as a simple and easy approach to implement. However, PD scheme leads to a steady state error, which can be reduced by increasing the proportional and the derivative gains. Nevertheless, the actuators can be damaged or suffer from saturation [2]. To overcome this issue, PID controller was proposed instead of PD technique. However, another problem represented in the stability is appeared, for which it can guarantee only locally [3]. This problem was solved in [4], where the author proved the global asymptotic stability of the PID controller under some complex conditions. After that, other control strategies based on the dynamic model have

* Corresponding author: chemseddine.boudjedir@g.enp.edu.dz

been developed such as computed torque controller (CT) and feedforward controller. The CT utilises the dynamic model with the actual position, velocity, and acceleration. Whereas, the FF controller utilises the dynamic model with the desired position, velocity, and acceleration. A comparative study was made between the two approaches for the trajectory tracking of the MIT serial arm [5]. The authors concluded that the two controllers have similar performances with a slight advantage to PD plus FF compensation represented in the ability to calculate the controller off-line.

The PD plus FF scheme was extensively studied in the last three decades. Indeed, the above-mentioned method was implemented successfully in many robots such as the direct-drive vertical arm [6], the MIT serial arm [7], and the COMAU robot [8]. It has been shown through experimental results that the PD plus FF compensation can improve the performance compared to the case when the PD works alone. The convergence analysis of the PD plus FF was proven in [6], where the control gains need to satisfy some constraints to achieve the global asymptotic stability of the closed-loop system. The drawback of the FF compensation is related to the fact that the design approach is based on the knowledge of the exact dynamic model, which is not an easy task. For instance, the frictions have an important effect on the dynamic model that is generally not taken properly into account. Another issue represented in the use of the matrix of centrifugal and Coriolis forces which contains quadratic terms of the joint velocities. This latter may introduce high-order non-linearities into the controller and drive the actuators to saturation, especially at high accelerations which is the case of the Delta robot.

In recent times, many repetitive tasks have been integrated into the industry such as pick and place operations [9], laser cutting [10] and chemical process [11]. To benefit from this repetition, Arimoto et al developed in 1984 an ILC scheme [12]. The main idea of ILC is to store the tracking errors of the previous iterations and then use them to improve the tracking error of the actual iteration. Several ILC strategies have been proposed in the literature in order to deal with the different needed tasks [13]-[16]. In [17, 18], the author presented an adaptive ILC to handle the parametric and non-parametric uncertainties effects. A robust ILC was discussed in [19] to deal with the same issue. In [20], the authors suggested a PD feedback controller plus PD-type ILC for trajectory tracking of a parallel Delta robot, where the convergence analysis was proven under the practical alignment condition.

The aim of this study is to evaluate the efficiency and the performance of the ILC scheme over the FF compensation under a repetitive environment. To this end, an experimental comparative study between the PD plus ILC and the PD plus FF is conducted. The two controllers are implemented on a parallel Delta robot (ISIR 88) containing a gear reducer that generates frictions. Experimental results show good tracking performance of the controllers and point out the superiority of the model-free ILC over the model-based FF through the iterations.

The rest of this paper is organised as follows. The dynamic model of the parallel Delta robot is described in Section 2. In section 3, PD plus FF controller and PD plus ILC controller are presented. The results of the experiment are provided in Section 4. Section 5 summarises this paper.

2 Dynamic model of parallel Delta robot

The parallel Delta robot illustrated in Fig. 1 consists of three identical kinematic chains, travelling plate, a fixed base, and a telescopic arm connects the travelling plate and the fixed base. The Delta robot has a very important friction due to the existence of a gear reducer between the brushless DC motor and the arms. This friction has a sustained effect, and as it is not taken into account in the dynamic model, the performance of the controllers

that based on the dynamic model can be degraded considerably. For a comprehensive review, a study on the effects of gear reduction on robot dynamics can be found in [21].

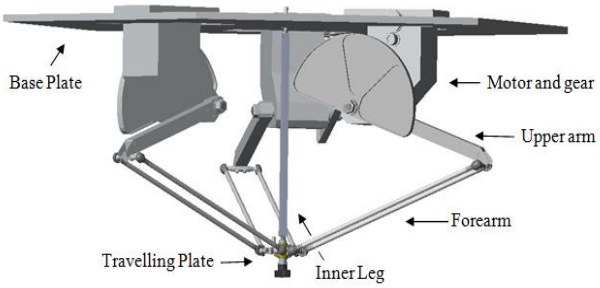

Fig. 1 The delta robot.

The inverse dynamic model of the parallel Delta robot is derived based on the principle of virtual work [22]. Its expression is given as follows:

$$M(q)\ddot{q} + C(q,\dot{q})\dot{q} + G(q) = \tau \quad (1)$$

Where:

$$\mathrm{M(q)} = \mathrm{I_b} + \mathrm{m_{nt}J^TJ}$$
$$\mathrm{C(q,\dot{q})} = \mathrm{J^T m_{nt}\dot{J}}$$
$$\mathrm{G(q)} = -\tau_{\mathrm{Gn}} - \tau_{\mathrm{Gb}}$$

and $\mathrm{q} = [\mathrm{q_1}, \mathrm{q_2}, \mathrm{q_3}]^{\mathrm{T}}$ is the generalized joint vector, $\mathrm{M(q)} \in \mathbb{R}^{3\times3}$ is the inertia matrix, $\mathrm{C(q,\dot{q})\dot{q}} \in \mathbb{R}^{3\times3}$ is the vector of Coriolis and centripetal torques, $\mathrm{G(q)} \in \mathbb{R}^3$ is the Gravity vector, τ is the joint torque vector, $\tau_{\mathrm{Gb}} \in \mathbb{R}^3$ is the torque vector produced by the gravitational force of the arms, $\tau_{\mathrm{Gn}} \in \mathbb{R}^3$ is the torque vector produced by the inertial force. J represents the Jacobian matrix and $\dot{\mathrm{J}}$ is its time derivative, $\mathrm{m_{nt}}$ represents the total mass. The expression of τ_{Gb} and τ_{Gn} is given by:

$$\tau_{\mathrm{Gb}} = \mathrm{m_b r_{Gb} g[cosq_1 \quad cosq_2 \quad cosq_3]^T} \quad (2)$$

$$\tau_{\mathrm{Gn}} = \mathrm{J^T m_{nt}[0 \quad 0 \quad -g]^T} \quad (3)$$

The detailed expressions of the Jacobian J, $\dot{\mathrm{J}}$, and $\mathrm{m_{nt}}$ are given in [22]. The geometrical and dynamic parameters of the Delta robot are presented in Table 1.

Table 1. Geometric and dynamic parameters

Parameter	Description	Value
L_A	Length of upper arm	0.205 m
L_B	Length of forearm	0.380 m
m_n	Mass of the travelling plate	0.042 kg
m_{br}	Mass of the upper arm	0.098 kg
m_{fb}	Masses of the forearms	0.028 kg
m_c	Mass of the elbow	0.015 kg

3 Controller design

In this section, we present the proposed controllers for the parallel Delta robot.

3.1 Controllers expression

The PD plus feedforward compensation expression is given by:

$$\tau_k = K_p\tilde{q}_k + K_d\dot{\tilde{q}}_k + M(q_d)\ddot{q}_d + C(q_d,\dot{q}_d)\dot{q}_d + G(q_d) \quad (4)$$

The PD plus PD-type ILC algorithm is given as follows:

$$\tau_k = K_p\tilde{q}_k + K_d\dot{\tilde{q}}_k + u_k \quad (5)$$

$$u_{k+1} = u_k + \Lambda\tilde{q}_k + \Gamma\dot{\tilde{q}}_k \quad (6)$$

In which, $\tilde{q}_k = q_d - q_k$ and $\dot{\tilde{q}}_k = \dot{q}_d - \dot{q}_k$, are the joint position and velocity error respectively. The index k denotes the iteration number, q_d and $\dot{q}_d$ represent the desired joint position and the desired joint velocity respectively. K_p, K_d, Γ, and Λ are positive definite diagonal matrices.

The schemes of the proposed controllers are illustrated in Fig. 2 and Fig. 3 respectively. In which, x_d represents the desired trajectory in the task space and IGM indicates the inverse geometric model.

As it can be seen, the two strategies compose of two parts: a PD feedback control plus a feedforward compensation. For the first strategy, the feedforward compensation is represented in the desired torque, which is extracted from the desired planned trajectory. For the second strategy, the feedforward compensation is represented in the PD-type ILC, which utilises the errors of the previous cycles. It is clear that the PD plus ILC has more simple structure and an easy algorithm to implement compared to the PD plus FF.

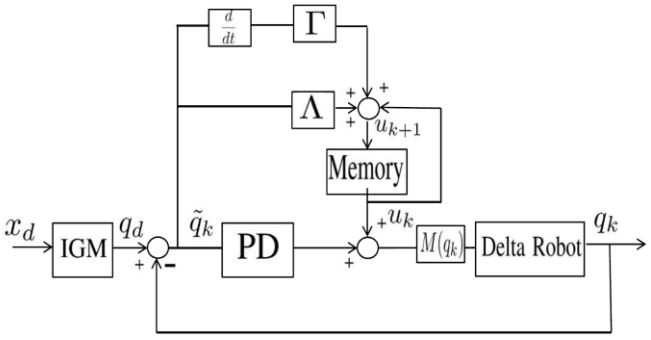

Fig. 2. The PD plus ILC control scheme.

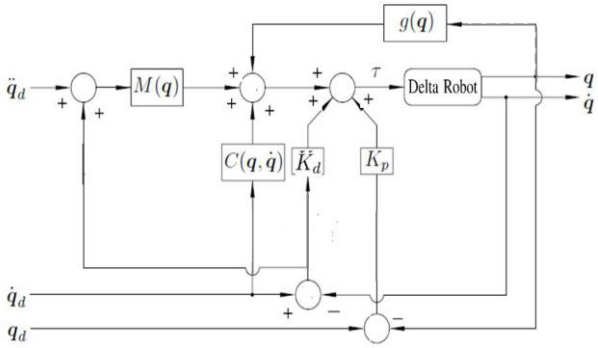

Fig. 3. The PD plus FF control scheme.

3.2 Relationship between PD plus FF and PD plus ILC

In this part, we explain the relationship between the PD plus FF controller and the PD plus ILC controller. To this end, let us consider the perfect dynamic model of the Delta robot where the external disturbances and the frictions are not taken into account. On one hand, by applying the PD plus FF torque we obtain:

$$\begin{aligned} M(q)\ddot{q} + C(q,\dot{q})\dot{q} + G(q) = \quad & K_p\tilde{q}_k + K_d\dot{\tilde{q}}_k \\ & + M(q_d)\ddot{q}_d + C(q_d,\dot{q}_d)\dot{q}_d + G(q_d) \end{aligned} \tag{7}$$

If the control gains are chosen as in [6], then the position and velocity tracking errors will converge asymptotically to zero. So on, the torque will converge asymptotically to FF control, ie:

$$\tau \to M(q_d)\ddot{q}_d + C(q_d,\dot{q}_d)\dot{q}_d + G(q_d) \quad as \quad t \to \infty$$

On the other hand, by applying the PD plus ILC torque we obtain

$$M(q)\ddot{q} + C(q,\dot{q})\dot{q} + G(q) = K_p\tilde{q}_k + K_d\dot{\tilde{q}}_k + u_k \tag{8}$$

If the control gains are chosen as in [20], then the position and velocity tracking errors will converge asymptotically to zero. So on, the torque will converge asymptotically to the ILC control which will converge asymptotically to FF control, ie:

$$\tau \to u_k \to M(q_d)\ddot{q}_d + C(q_d,\dot{q}_d)\dot{q}_d + G(q_d) \quad as \quad t \to \infty$$

As a conclusion, the ILC will converge to the FF after a certain time, which means that the performances of the FF will be better than the ILC. This is can be explained by the fact that the FF torque starts from the same desired torque obtained for perfect tracking while the ILC torque starts from a random value then converges to the desired torque.

Next, let us consider the real dynamic model of the Delta robot, where its expression is given as follows:

$$M(q)\ddot{q} + C(q,\dot{q})\dot{q} + G(q) + d(t) = \tau \qquad (9)$$

In which, $d(t)$ represents the external disturbances and frictions.

The main question here is this: Under a repetitive trajectory, do the performances of the FF remain better than those of ILC despite the influence of the gear reducer and other external disturbances on the robot dynamics?

4 Experimental results

In this section, we present the experimental results obtained by applying the proposed controllers on the parallel Delta illustrated in Fig. 4.

Fig. 4. Delta robot experimental platform

The proposed controllers are implemented into a PC running at 2.8 GHz, using a real-time extension (RTX) from IntervalZero loaded in Windows XP. The robot is equipped with three brushed DC motors (UGTMEM-03LB2), with a belt-driven transmission of ration 12. The control algorithms are programmed with the C language and executed with a sampling time of 1 ms.

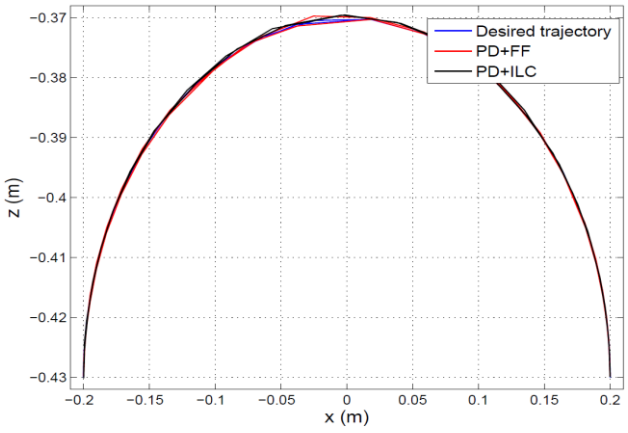

Fig. 5. Experimental task space.

The desired reference is semi-elliptic trajectory realized using a parabolic position profile and a maximal acceleration of 10 m/s^2. The desired trajectory starts from the initial position $(0.20,0,-0.43)$m to the final position $(-0.20,0,-0.43)$m and returns to the initial position during 0.88 second.

The PD controller gains were chosen as: $K_p = \text{diag}\{2.2\}$, $K_d = \text{diag}\{0.0145\}$, and the ILC controller gains were set to $\Lambda = \text{diag}\{0.074\}$, $\Gamma = \text{diag}\{0.0015\}$. The Root Mean Square Error (RMSE) criteria expressed by (10) is used to evaluate the tracking performance of the controllers.

$$\text{RMSE} = \sqrt{\frac{1}{n}\sum_{i=1}^{n}(q_i - q_{d_i})^2} \qquad (10)$$

Where q_{d_i} is the desired trajectory, q_i is the actual response, and n is the total number of samples in one iteration.

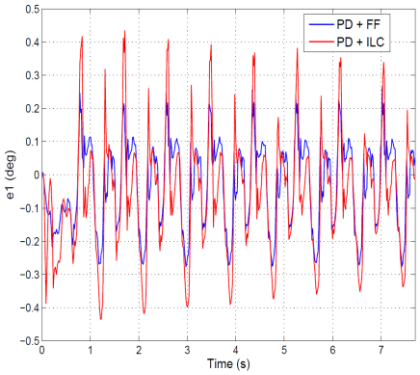

Fig. 6. Experimental tracking errors of joint 1 for k=1-8.

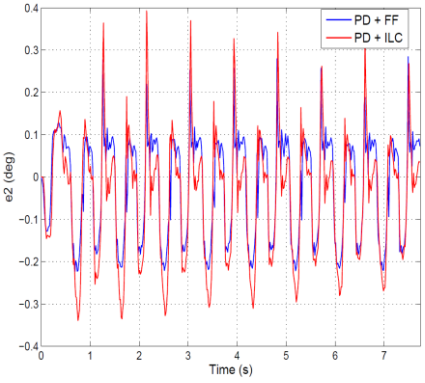

Fig. 7. Experimental tracking errors of joint 2 for k=1-8.

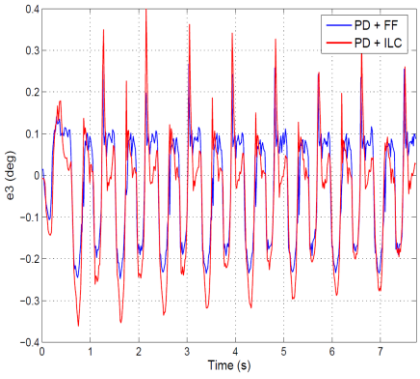

Fig. 8. Experimental tracking errors of joint 3 for k=1-8.

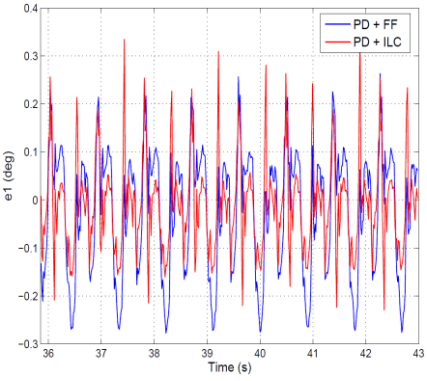

Fig. 9. Experimental tracking errors of joint 1 for k=41-48.

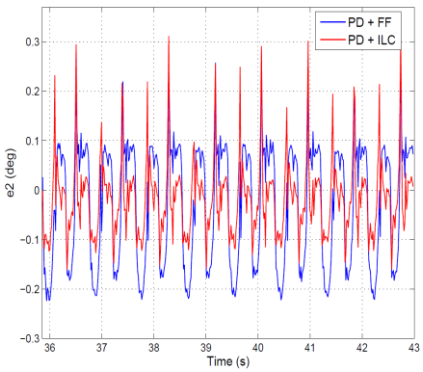

Fig. 10. Experimental tracking errors of joint 2 for k=41-48.

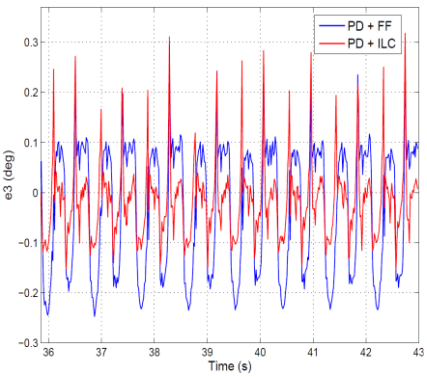

Fig. 11. Experimental tracking errors of joint 3 for k=41-48.

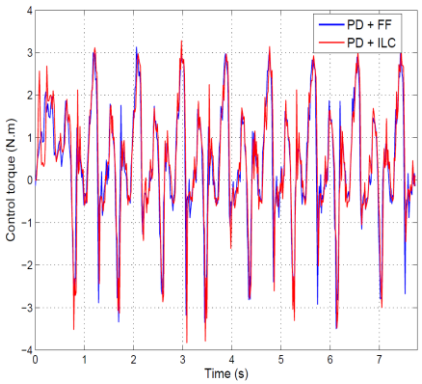

Fig. 12. Experimental control torque of joint 1 for k=1-8

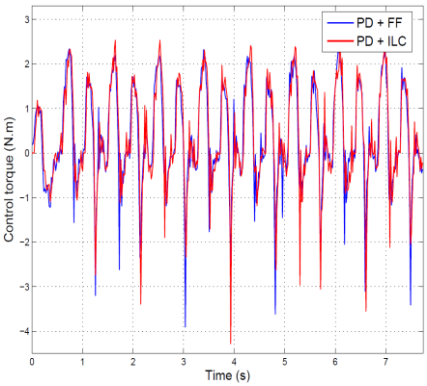

Fig. 13. Experimental control torque of joint 2 for k=1-8

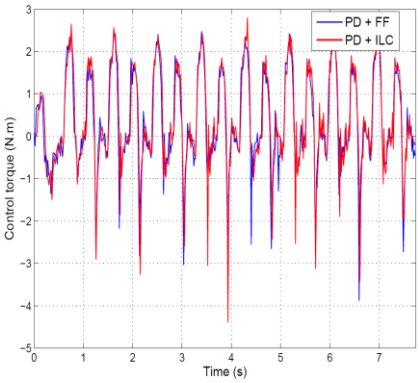

Fig. 14. Experimental control torque of joint 3 for k=1-8

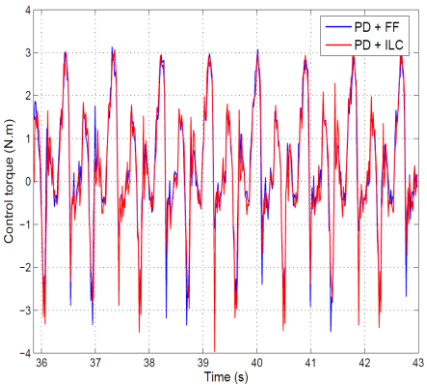

Fig. 15. Experimental control torque of joint 1 for k=41-48

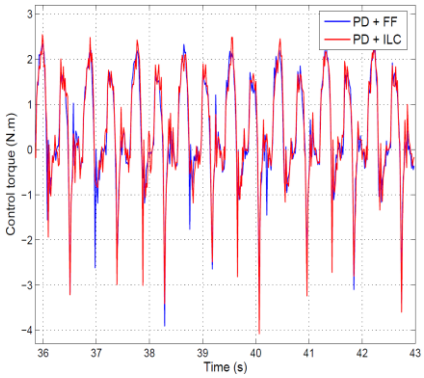

Fig. 16. Experimental control torque of joint 2 for k=41-48

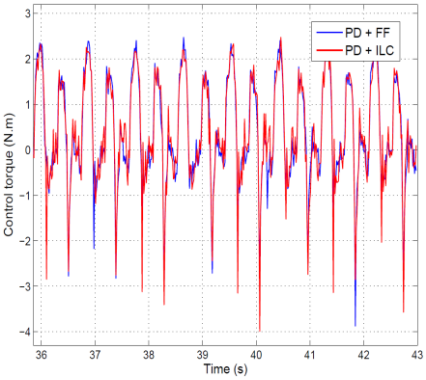

Fig. 17. Experimental control torque of joint 3 for k=41-48

Fig. 5 shows the experimental tracking trajectory in the task space under the PD plus FF compensation and the PD plus ILC respectively. Fig. 6, Fig. 7, and Fig. 8 depict the tracking error under the proposed controllers of the first eight iterations of joint 1, joint 2 and joint 3 respectively (the tracking error of joint 3 is similar to the joint 2 due to the nature of the trajectory). It is observed that, on one hand, the tracking error of the PD plus FF is smaller than the PD plus ILC. On the other hand, the tracking error of the PD plus ILC decreases from iteration to iteration.

Fig. 9, Fig. 10, and Fig. 11 present the tracking error of iterations 41 to 48 of joint 1, joint 2 and joint 3 respectively. As it can be seen, the performance of the PD plus ILC becomes better through the iterations than the PD plus FF. Fig. 12 to Fig. 17 show the control torque signals for the proposed controllers through the iterations. It is observed that the two controllers have nearly the same variation and magnitude for the first and the last eight iterations. Fig 18 indicates the progress of the RMSE through the iterations which are summarised in Table 2.

It can be concluded that, at the beginning the FF has superior performance than the ILC. However, the performance of the ILC becomes better than the FF through the iterations. This is can be explained by the fact that the performance of the model-based PD plus FF controller is influenced by the frictions of the gear and the lack of the exact dynamic model, whereas, the performance of the model-free PD plus ILC continues to improve from iteration to iteration using only the information of the previous cycles.

Table 2. The tracking performances

Iteration		1	10	30	40	48
RMSE PD+FF (mm)	x-axis	0.49	0.48	0.47	0.48	0.47
	z-axis	0.43	0.42	0.42	0.43	0.42
RMSE PD+ILC (mm)	x-axis	0.81	0.48	0.39	0.37	0.38
	z-axis	0.58	0.41	0.29	0.30	0.31

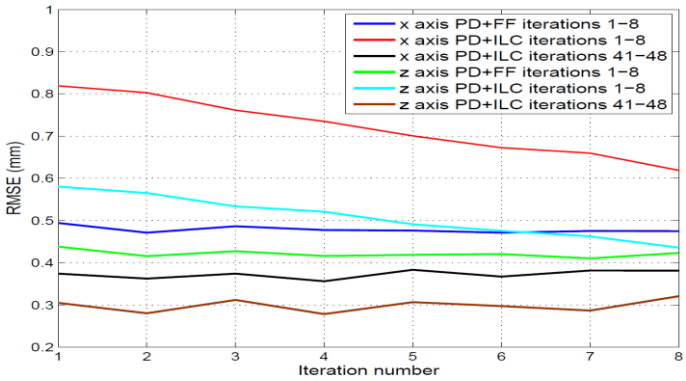

Fig. 18. Experimental RMSE

5 Conclusion

This work presented a comparative study between PD plus FF compensation and PD plus ILC controller with application to a parallel Delta robot performing repetitive trajectory. As the FF compensation utilises the robot dynamic model without taking into account the friction model, the performance of the FF can be degraded significantly. To overcome this issue, a model-free PD-type ILC was introduced instead of the FF compensation. Experimental results show that the tracking performance of the PD plus ILC converges towards the tracking performance of the PD plus FF and eventually surpasses it through the iterations with similar torques.

This work was supported by the Laboratory Biorobotics/ Ecole Polytechnique Fédérale de Lausanne (BIOROB/EPFL), and the General Directorate of Scientific Research and Technological Development/Ministry of High Education and Scientific Research of Algeria (DGRSDT/MESRS).

References

1. C. E. Boudjedir, D. Boukhetala, and M. Bouri, Journal of Electrical Engineering. **69**, 329-336 (2018).
2. R. Kelly, V. Santibáñez, and A. Loría, Control of Robot Manipulators in Joint Space, (Springer, Berlin, 2005)
3. R. Kelly, Robotica. **13**, 141–148 (1995).
4. S. Arimoto, Control theory of non-linear mechanical systems, (Oxford, UK: Oxford Science Publications, 1996).
5. C.H. An, C.G. Atkeson, J.D. Griffiths, and J.M. Hollerbach, IEEE Trans. on Robotics and Automation. **5**, 368–373 (1989).
6. V. Santibañez and R. Kelly, Robotica. **19**, 11–19 (2001).
7. C. H. An, C. G. Atkeson, and J. M. Hollerbach, in Proc. IEEE Int. Conf. Robotics and Automation, 55–60, San Francisco, USA (1986).
8. F. Caccavale and P. Chiacchio, Control Engineering Practice. **2**, 1039–1050 (1994).
9. C. E. Boudjedir, D. Boukhetala, and M. Bouri, IEEE Transactions on Industrial

Electronics. **68**, 7433-7443 (2021).

10. C. H. Tsai and C. J. Chen, Opt. Laser Eng. **41,** 189–204 (2004).
11. J. W. Choi, H. G. Choi, K. S. Lee, and W. H. Lee, Journal of Biotechnology. **49**, 29-43 (1996).
12. S. Arimoto, S. Kawamura, and F. Miyazaki, in: H. Hanafusa, H. Inoue (Eds.), Robotics Research, Second International Symposium, MIT Press, 127–134 Cambridge (1984).
13. C. E. Boudjedir, D. Boukhetala, and M. Bouri, in 5th International conference on electrical engineering, 1-6, Boumerdès, Algeria (2017).
14. C. E. Boudjedir, D. Boukhetala, and M. Bouri, Nonlinear Dynamics. **95**, 2197-2208 (2019).
15. C. E. Boudjedir, D. Boukhetala, and M. Bouri, In: Chadli M., Bououden S., Ziani S., Zelinka I. (eds) Advanced Control Engineering Methods in Electrical Engineering Systems. Lecture Notes in Electrical Engineering, **522** (Springer, 2017).
16. C. E. Boudjedir, D. Boukhetala, and M. Bouri, in International Conference on Electrical Sciences and Technologies in Maghreb (CISTEM), 1-4, Algiers, Algeria (2018).
17. A. Tayebi, Automatica. **40**, 1195–1203 (2004).
18. C. E. Boudjedir and D. Boukhetala, Proceedings of the Institution of Mechanical Engineers, Part I: Journal of Systems and Control Engineering. **235**, 207-221 (2021).
19. X. Li, D. Huang, B. Chu, and J. X. Xu, Int. J. Robust Nonlinear Control, **26** 697-718 (2015).
20. C. E. Boudjedir, M. Bouri, and D. Boukhetala, at – Automatisierungstechnik. **67**, 145-156 (2019).
21. J. Chen, Pasadena, CA. **4**, 297-307 (1989).
22. A. Codourey, In: Proceedings of IEEE/ RSJ international conference on intelligent robots and systems. **3**, 1211–8 (1996).